Estudos (Inter) Multidisciplinares nas Ciências Exatas e Tecnologias

Henrique Ajuz Holzmann
João Dallamuta
Ricardo Vinicius Bubna Biscaia
(Organizadores)

Atena Editora
Ano 2019

Estudos (Inter) Multidisciplinares nas Ciências Exatas e Tecnologias

Henrique Ajuz Holzmann
João Dallamuta
Ricardo Vinicius Bubna Biscaia
(Organizadores)

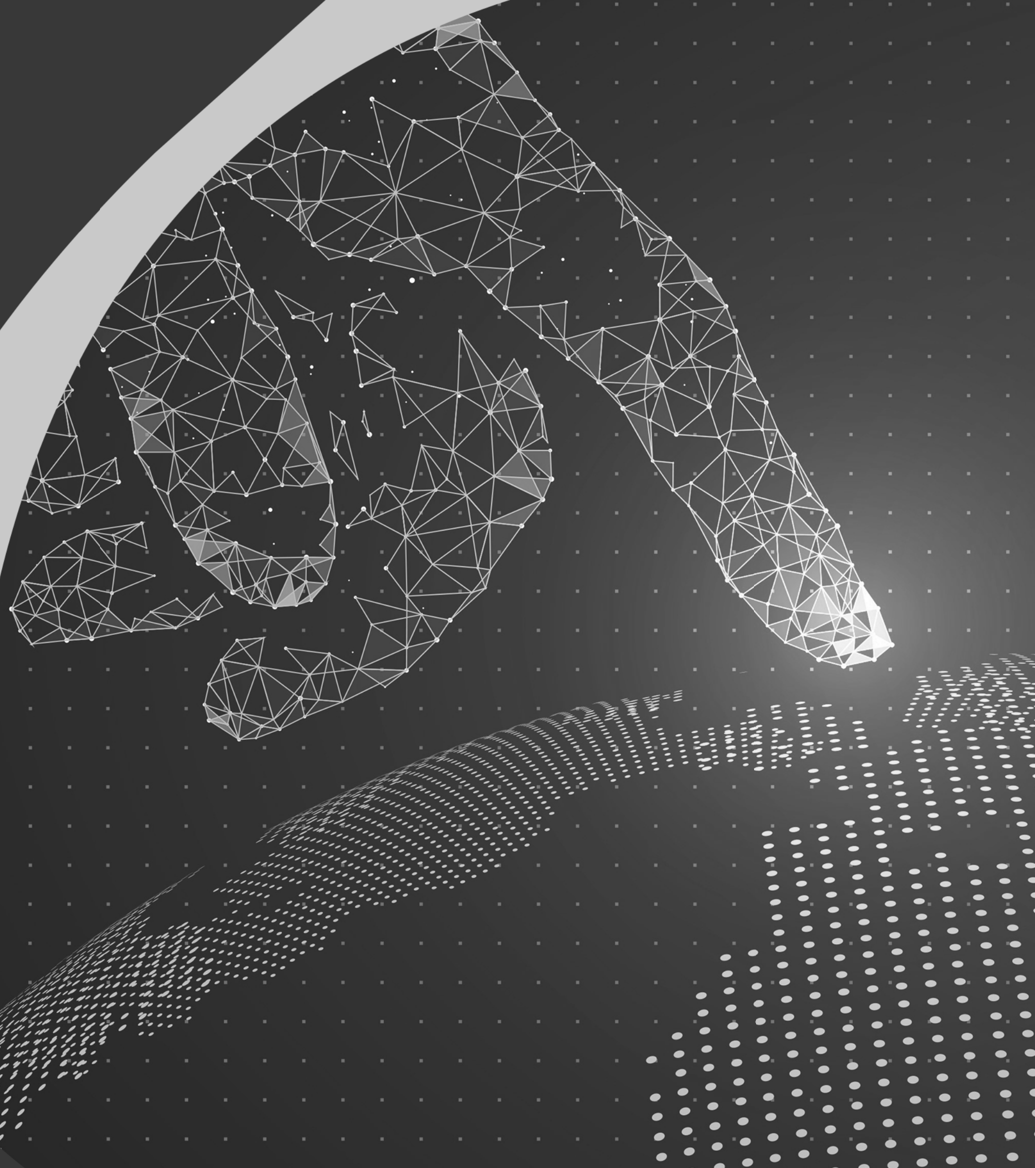

Atena Editora
Ano 2019

2019 *by Atena Editora*
Copyright © Atena Editora
Copyright do Texto © 2019 Os Autores
Copyright da Edição © 2019 Atena Editora
Editora Chefe: Profª Drª Antonella Carvalho de Oliveira
Diagramação: Lorena Prestes
Edição de Arte: Lorena Prestes
Revisão: Os Autores

Dados Internacionais de Catalogação na Publicação (CIP)
(eDOC BRASIL, Belo Horizonte/MG)

E82 Estudos (inter) multidisciplinares nas ciências exatas e tecnologias [recurso eletrônico] / Organizadores Henrique Ajuz Holzmann, João Dallamuta, Ricardo Vinicius Bubna Biscaia. – Ponta Grossa, PR: Atena Editora, 2019.

Formato: PDF
Requisitos de sistema: Adobe Acrobat Reader.
Modo de acesso: World Wide Web.
Inclui bibliografia
ISBN 978-85-7247-798-7
DOI 10.22533/at.ed.987192611

1. Ciências exatas – Pesquisa – Brasil. 2. Tecnologia. I.Holzmann, Henrique Ajuz. II. Dallamuta, João. III. Biscaia, Ricardo Vinicius Bubna.

CDD 509

Elaborado por Maurício Amormino Júnior – CRB6/2422

Atena Editora
Ponta Grossa – Paraná - Brasil
www.atenaeditora.com.br
contato@atenaeditora.com.br

Atena Editora
Ano 2019

APRESENTAÇÃO

Neste livro são apresentados vários trabalhos, alguns com resultados práticos, outros com métodos de desenvolvimento para o ensino de tecnologias, bem como um enfoque em energias renovais.

Um compendio de temas e abordagens que constituem a base de conhecimento de profissionais que buscam estar atualizados e alinhados com as novas tecnologias .

A obra Estudos (Inter) Multidisciplinares nas Ciências Exatas e Tecnologias aborda os mais diversos assuntos sobre a aplicação de métodos e ferramentas nas diversas áreas das engenharias a fim de melhorar a relação ensino aprendizado, sendo por meio de levantamentos teórico-práticos de dados referentes aos cursos ou através de propostas de melhoria nestas relações.

Outro ponto de grande destaque, são as novas ferramentas utilizadas em um compendio relacionado ao ensino-aprendizagem, como ferramentas tecnológicas que facilitem o entendimento e executem um link entre aluno-professor-conteúdo.

Desta forma temas e abordagens que facilitam as relações entre ensino-aprendizado são apresentados, a fim de se levantar dados e propostas para novas discussões em relação ao ensino nas engenharias, de maneira atual e com a aplicação das tecnologias hoje disponíveis.

Boa leitura

Henrique Ajuz Holzmann
João Dallamuta
Ricardo Vinicius Bubna Biscaia

SUMÁRIO

CAPÍTULO 24

STRENGTH PREDICTION OF ADHESIVELY-BONDED JOINTS WITH COHESIVE LAWS ESTIMATED BY THE DIRECT METHOD

Ulisses Tiago Ferreira Carvalho
Instituto Superior de Engenharia do Porto
Porto – Portugal

Raul Duarte Salgueiral Gomes Campilho
Instituto Superior de Engenharia do Porto
Porto – Portugal

ABSTRACT: Cohesive Zone Models (CZM) are a powerful tool for the design of bonded structures, but they require careful estimation of the cohesive laws for reliable results. This work experimentally evaluates by the J-integral/direct method the tensile and shear CZM laws of three adhesives with distinct ductility. Additionally, by the direct method, the precise shape of the cohesive law in tension and shear of the adhesives is defined. The Double-Cantilever Beam (DCB) and End-Notched Flexure (ENF) specimens were considered to obtain the tensile and shear CZM laws of the adhesives, respectively. After obtaining the tensile and shear CZM laws, triangular, exponential and trapezoidal CZM laws were built to reproduce their behaviour. Validation of these CZM laws was undertaken with a mixed-mode geometry (double-lap joint) considering the same three adhesives and varying overlap lengths (LO). The strength prediction by this technique revealed accurate predictions for a given CZM law shape, depending on the adhesive ductility, although all CZM law shapes were moderately accurate.

KEYWORDS: Adhesive joint; Structural adhesive; Cohesive zone models; Strength prediction.

PREVISÃO DE RESISTÊNCIA DE JUNTAS ADESIVAS COM LEIS COESIVAS ESTIMADAS PELO MÉTODO DIRETO

RESUMO: Os modelos de dano coesivo (MDC) são uma ferramenta poderosa para o projeto de ligações adesivas, mas requerem uma estimativa cuidadosa das leis coesivas para obter resultados precisos. Este trabalho avalia experimentalmente, pelo método do integral J/método direto, as leis coesivas à tração e corte de três adesivos com ductilidade distinta. Além disso, pelo método direto, é definida a forma precisa da lei coesiva em tensão e corte dos adesivos. Foram utilizados provetes Double-Cantileve Beam (DCB) e End-Notched Flexure (ENF) para a obtenção das leis coesivas de tração e corte dos adesivos, respetivamente. Após a obtenção destas leis coesivas, foram construídas leis aproximadas triangulares, exponenciais e trapezoidais para reproduzir o seu comportamento. A validação destas leis coesivas foi realizada com uma geometria de modo misto (junta de sobreposição dupla) considerando os mesmos três adesivos e comprimentos de sobreposição (LO) variáveis.

A previsão da resistência por esta técnica revelou resultados precisos para uma determinada forma de lei coesiva, dependendo da ductilidade do adesivo, embora todas as formas de leis coesivas fossem moderadamente precisas.

PALAVRAS-CHAVE: Junta adesiva; Adesivo estrutural; Modelos de dano coesivo; Previsão de resistência.

1 I INTRODUCTION

There is a countless number of joint configurations addressed in the literature, although the most common are single-lap, double-lap and scarf joints (Li et al., 2015). The availability of accurate and straight-forward predictive methods is thus mandatory for the safe design of bonded joints. Although several techniques have been proposed for many decades, beginning with the theoretical analysis of Volkersen (1938), the Continuum mechanics criteria coupled to a Finite Element Analysis (FEA), Linear Elastic Fracture Mechanics (LEFM) or the CZM. CZM been refined ever since were initially proposed some decades ago, to become nowadays a very powerful technique for damage growth and strength prediction of structures, including the analysis of wood failure (Campilho et al., 2010), composite delaminations (Alfano e Crisfield, 2001; Jiang et al., 2007) and bonded joint analysis (Goyal et al., 2008; Campilho et al., 2011), for which this technique is particularly suited (Fernandes et al., 2015). While CZM is a powerful technique to predict the strength of bonded joints, some premises must be accounted for to ensure reliable results: the adhesive should be characterized under identical geometrical conditions in which the resulting laws will be used in the simulations, and the stipulated CZM law shape should be consistent with the adhesive's behaviour (Campilho et al., 2008).

Different techniques are nowadays available for the definition of the cohesive parameters (GIC, GIIC, t_n^0 and t_s^0), such as the property identification technique, the direct method and the inverse method. The direct method, which is the purpose of this work, gives the precise shape of the CZM laws of a specific material or interface, since these are estimated from the experimental data of fracture tests such as the DCB or ENF (Pandya e Williams, 2000). This is done by differentiation of the tensile strain energy release rate, GI, for tension, or the shear strain energy release rate, GII, for shear, with respect to the relative opening of the crack (δn for tension or δs for shear). Nonetheless, it is usual to convert the obtained shape to an approximated parameterized shape for introduction in the FEA software. For an accurate measurement of the required parameters such as δn or δs, physical sensors (Ji et al., 2010) or image correlation methods (Han e Siegmund, 2012; Valoroso et al., 2013) can be used. The validity of the direct approach can be checked by numerically replicating the tensile or shear fracture tests with identical dimensions and with the experimentally obtained CZM laws as input for the adhesive layer's behaviour, followed by comparing the obtained P-δ curves with the original ones from the experiments (Valoroso et al., 2013). However, complete validation of the CZM laws should include testing the pure mode CZM laws in a mixed-mode geometry, although to the authors' knowledge such works are not available in the literature, being these works limited to pure-mode verifications.

This work experimentally evaluates by the J-integral/direct method the tensile and shear CZM laws of three adhesives with distinct ductility. Additionally, by the direct method, the precise shape of the cohesive law in tension and shear of the adhesives is defined. The DCB and ENF specimens were considered to obtain the tensile and shear CZM laws of the adhesives, respectively. After obtaining the tensile and shear CZM laws, triangular, exponential and trapezoidal CZM laws were built to reproduce their behaviour. Validation of these CZM laws was undertaken with a mixed-mode geometry (double-lap joint) considering the same three adhesives and varying L_O values.

2 I EXPERIMENTAL WORK

2.1 Materials

For the DCB, ENF and double-lap specimens, the high strength and ductile aluminium alloy AA6082 T651 was chosen for the adherends. The tensile mechanical properties of this material were obtained in the work of Campilho et al. (2011). The experimental testing programme included three structural adhesives: the brittle epoxy Araldite® AV138, the ductile epoxy Araldite® 2015 and the ductile polyurethane Sikaforce® 7752. In this manner, different material behaviours are tested. These adhesives were previously characterized regarding the mechanical and toughness properties (Campilho et al., 2011; Campilho, Banea, et al., 2013; Faneco et al., 2015). Bulk specimens were tested in a servo-hydraulic machine to obtain Young's modulus (E), σy, σf and ξf. The DCB test was selected to obtain GIC and the ENF test was used for GIIC. The collected data of the adhesives is summarized in Table 1.

Property	AV138	2015	7752
Young's modulus, E [GPa]	4.9±0.8	1.9±0.2	0.5±0.1
Poisson's ratio, *ν*	0.35 a	0.33 a	0.30 a
Tensile yield stress, σ_y [MPa]	36.5±2.5	12.6±0.6	3.2±0.5
Tensile failure strength, σ_f [MPa]	39.5±3.2	21.6±1.6	11.5±0.3
Tensile failure strain, ε_f [%]	1.2±0.1	4.8±0.8	19.2±1.4
Shear modulus, G [GPa]	1.6±0.01	0.6±0.2	0.2±0.01
Shear yield stress, τ_y [MPa]	25.1±0.3	14.6±1.3	5.2±1.1
Shear failure strength, τ_f [MPa]	30.2±0.4	17.9±1.8	10.2±0.6
Shear failure strain, γ_f [%]	7.8±0.7	43.9±3.4	54.8±6.4
Toughness in tension, GIC [N/mm]	0.20 b	0.4±0.02	2.4±0.2
Toughness in shear, GIIC [N/mm]	0.38 b	4.7±0.3	5.4±0.5
a manufacturer's data			
b estimated in Campilho et al. (2011)			

Table 1. Properties of the adhesives Araldite® AV138, Araldite® 2015 and Sikaforce® 7752 (Campilho et al., 2011; Campilho, Banea, et al., 2013; Faneco et al., 2015).

2.2 Joint Geometries

Fig. 1 shows the geometry and characteristic dimensions of the DCB (a) and ENF specimens (b). The chosen values for the dimensions are: total length L=140 mm (DCB) or mid-span L=100 mm (ENF), initial crack length a0≈50 mm, adherend thickness t_P=3 mm, t_A=0.2 mm and width B=25 mm. Fig. 2 describes the double-lap joints' geometry for validation of the obtained CZM laws, whose dimensions were the following: length between grips L_T=170 mm, t_P=3 mm, t_A=0.2 mm, L_O=12,5, 25, 37.5 and 50 mm and B=25 mm (not represented in the figure).

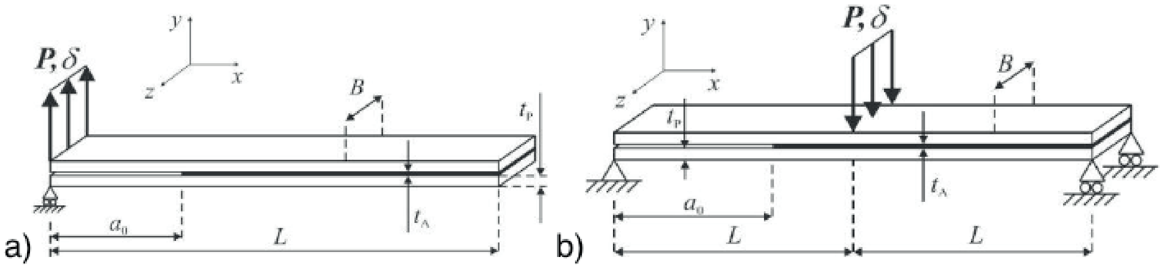

Fig.1 - DCB (a) and ENF (b) specimens for fracture characterization of thin adhesive bonds.

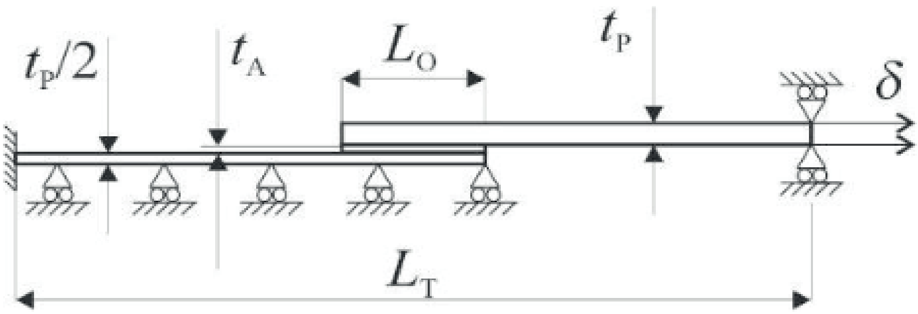

Fig.2 - Double-lap joint specimens for validation of the obtained CZM laws.

All joint configurations were fabricated and tested at room temperature. Joint tests were carried out in a Shimadzu AG-X 100 electro-mechanical testing machine with a 100 kN load cell. To apply the optical methods used in the DCB and ENF tests, images were recorded by an 18 MPixel digital camera with no zoom and fixed focal distance to approximately 100 mm, which enabled obtaining the values of a, δn, δs and adherends rotation at the specimen's loading point, θo, this last parameter required in the DCB tests for application of the J-integral.

2.3 Direct method for cohesive law estimation

Based on the fundamental expression for J (Rice, 1968), it is possible to derive an expression for GI (Eq.1) applied to the DCB specimen from the concept of energetic force and also the beam theory, as follows (Zhu et al., 2009)

$$G_I = 12\frac{(P_u a)^2}{E_x t_P^3} + P_u\theta_o \quad \text{or} \quad G_I = P_u\theta_p, \qquad (1)$$

where Pu represents the applied load per unit width at the adherends' edges and Ex is the adherends' value of E in the longitudinal direction. A schematic representation of δ_n, θ_o and θ_p, required by this method, is given in Fig. 3.

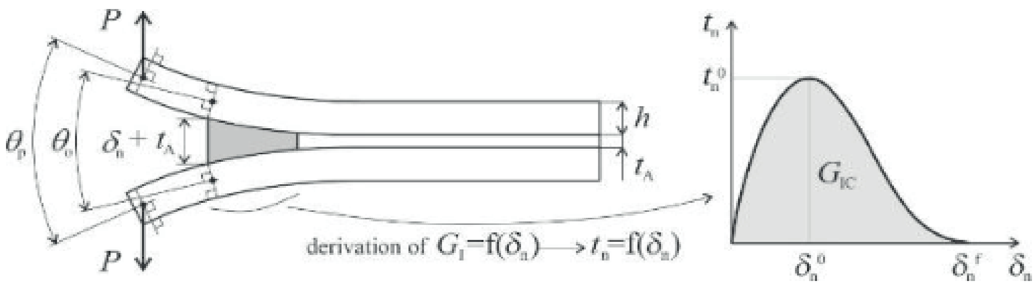

Fig.3 - DCB specimen under loading, with description of the analysis parameters, and estimation of the cohesive law.

In this figure, δ_n^0 is the relative displacement at t_n^0, and δ_n^f is the tensile failure displacement. The $t_n(\delta_n)$ or tensile CZM law is obtained by differentiation of equation (1) with respect to δ_n. More details about this technique applied to the DCB specimen can be found in reference (Campilho, Moura, et al., 2013). A developed algorithm to measure θ_o and δ_n was used (Campilho et al., 2014), based on digital image correlation and tracking reference points in the scales that follow crack growth during the test.

An identical procedure, i.e., based on the direct method, was used to evaluate GIIC and shear CZM law by the ENF test (Zhu et al., 2009; Campilho, Moura, et al., 2013), involving the concurrent measurement of the J-integral and δ_s. The GII expression (Eq.2) for the ENF specimen gives (Leffler et al., 2007)

$$G_{II} = \frac{9}{16}\frac{(P_u a)^2}{E_x t_p^3} + \frac{3}{8}\frac{P_u \delta_s}{t_p}. \qquad (2)$$

The t_s-δ_s curve (or shear CZM law) can then be assessed by differentiation of the G_{II}-δ_s curve. Full details regarding the description of the direct method applied to the ENF specimen, as well as the algorithm to estimate δ_s in every picture of a test, can be found in the work of Leitão et al. (2016).

3 I NUMERICAL ANALYSIS

3.1 Conditions of the numerical analysis

Geometrically non-linear analyses were considered for the double-lap joint models. The adherends were modelled as elasto-plastic continuum bodies and the adhesive was fully represented by a single layer of cohesive elements, i.e., by the continuum CZM approach (Campilho, Banea, et al., 2013). The models are two-dimensional, considering CPE4 plane-strain elements of Abaqus®. Apart from this, horizontal symmetry was applied to the double-lap joints. Fig. 4 shows a representative mesh for the CZM strength prediction analysis for a double-lap joint with L_O=25 mm. The FEA mesh included edge grading horizontally from the overlap inner portion towards the overlap edges, and vertically towards the adhesive layer, to increase the simulation speed, although keeping acceptable results. The joints were clamped at one edge and a vertical restraint and tensile displacement was applied at the opposite edge (Campilho et al., 2012).

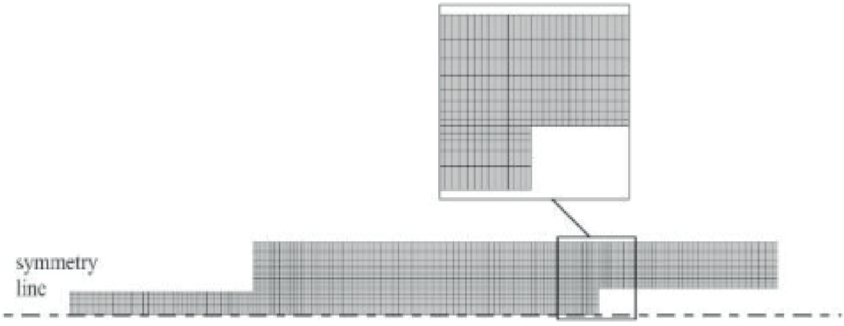

Fig.4 - Mesh detail for the LO=25 mm double-lap joint (CZM failure analysis).

3.2 CZM implementation in the FEA analysis

CZM are typically founded on a relationship between t_n/t_s and δ_n/δ_s that connects homologous nodes of the cohesive elements, to simulate the elastic behaviour up to t_n^0 (tension) or t_s^0 (shear) and subsequent material degradation up to final failure (Turon et al., 2007). In this work, the triangular, trapezoidal and linear-exponential shapes were evaluated to model the tensile and shear behaviour of the adhesive layer. Fig. 5 schematically represents these three CZM shapes with the associated nomenclature for both tensile and shear loadings (δ_s^0 the relative displacement at t_s^0, δ_s^f is the shear failure displacement, and dns and dss are the tensile and shear stress softening onset displacements of the trapezoidal CZM law, respectively). The definition of δ_n^s and δ_s^s is carried out by making GI=GIC for tension or GII=GIIC for shear (Turon et al., 2007).

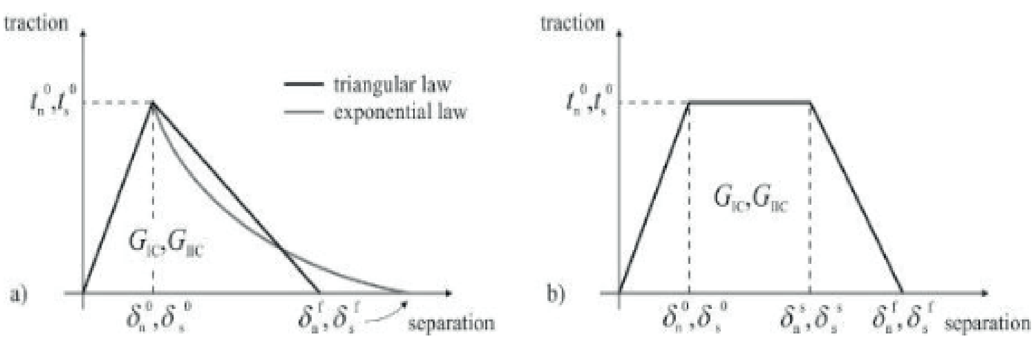

Fig.5 - CZM laws with triangular, linear-exponential and trapezoidal shapes available in Abaqus®.

Due to the unavailability in Abaqus® of mode coupling for the trapezoidal and exponential CZM laws, uncoupled loading modes were considered in all CZM simulations. This is supported by the findings of a previous work (Campilho, Banea, et al., 2013), in which it was found for composite single-lap joints that the results between mode-coupled and uncoupled predictions are virtually identical.

4 I RESULTS

4.1 GIC and GIIC evaluation by the fracture tests

All DCB and ENF specimens revealed a cohesive failure of the adhesive layer. The G_I-δ_n and G_{II}-δ_s curves were estimated from the direct method described in Section 2.3 using equations (1) and (2), respectively. Fig. 6 and Fig. 7 shows typical curves for the three adhesives and the DCB and ENF tests respectively, overlapped by polynomial approximation curves to apply the differentiation procedure leading to the definition of the respective CZM laws.

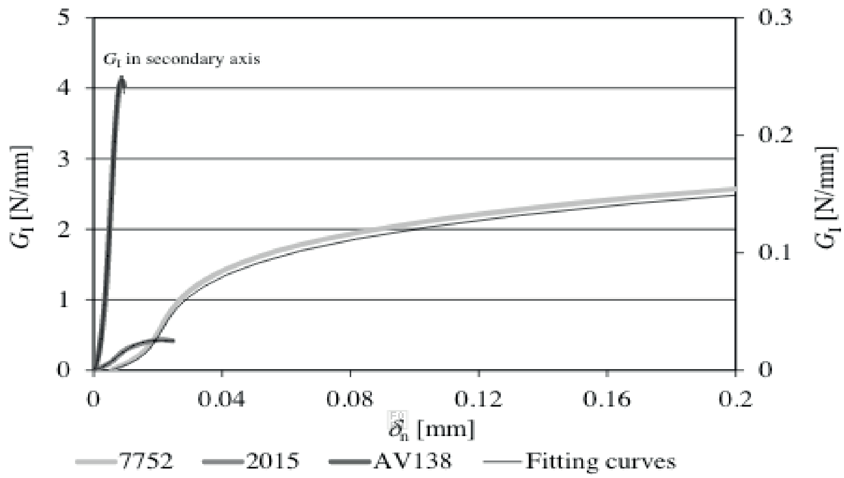

Fig.6 - Plot of G_I-δ_n for a specimen of each tested adhesive: raw curve and polynomial approximations.

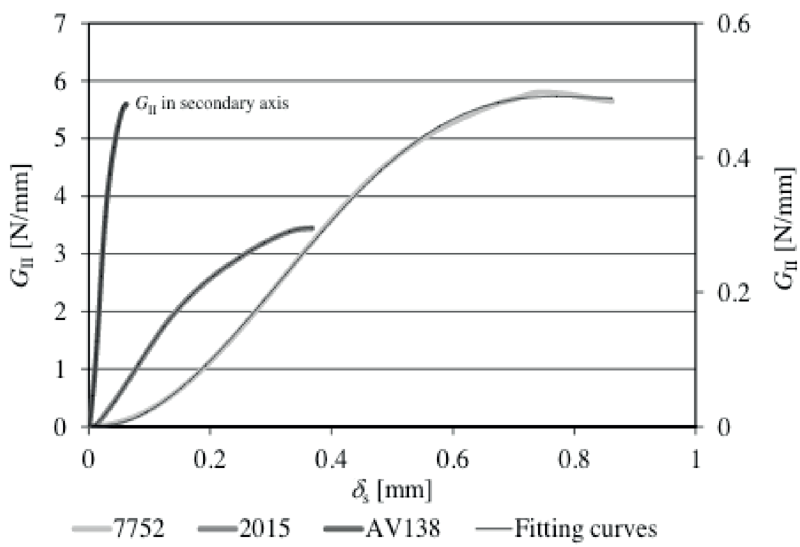

Fig.7 - Plot of G_{II}-δ_s for a specimen of each tested adhesive: raw curve and polynomial approximations.

In agreement with previous works (Jiang et al., 2007), three different stages can be identified in the G_I-δ_n and G_{II}-δ_s curves: (1) slow increase of GI/GII with δ_n/δ_s, (2) steady increase of GI/GII and (3) the curve tends to a steady-state value of GI/GII. The different behaviour between the three adhesives is clearly visible. The curves for each adhesive highly differ in terms of GIC/GIIC measurement and corresponding value of δ_n/δ_s, which corresponds to failure in the CZM law. GIC and GIIC are found by the steady-state values of GIC and GIIC in the respective curve and are attained at crack initiation (Ji et al., 2010). Table 2 reviews the GIC and GIIC values obtained by the J-integral for the three adhesives.

Adhesive	Araldite® AV138		Araldite® 2015		Sikaforce® 7752	
Specimen	GIC	GIIC	GIC	GIIC	GIC	GIIC
1	0.224	0.552	0.437	3.444	3.420	-
2	0.252	0.732	0.434	-	3.903	5067
3	0.231	0.676	0.494	2.873	3.842	6050
4	0.329	-	0.456	3.298	4.183	5360
5	0.237	0.566	0.665	3.123	-	6.07
6	0.197	0.533	0.712	3.140	3.502	5173
7	-	0.523	-	3.08	-	5790
8	-	0.479	-	2.901	-	6160
Average	0.245	0.580	0.533	3.123	3.770	5667
Deviation	0.045	0.09	0.123	0.203	0.278	0.459

Table 2. Values of GIC and GIIC [N/mm] for the three adhesives obtained by J-Integral technique (Azevedo et al., 2015; Campilho et al., 2015; Constante et al., 2015).

Fig. 8 presents a comparison between representative t_n-δn(a) and t_s-δ_s(b) curves for each of the adhesives (corresponding to the GI-δ_n and GII-δ_s curves of Fig. 6 and 7, respectively). Both tensile and shear CZM laws show that the Araldite®AV138 is bestfit by a triangular CZM law because of its brittle behaviour, whilst the Araldite®2015 and Sikaforce®7752 are modelled with trapezoidal CZM laws which, in this case, provide the best approximation on account of the plasticization endured after the initial elastic part of the curves. The different behaviour of these three adhesives under tension is consistent with the properties of the adhesives reported in Table 1, namely ε_f and GIC(tensile CZM laws) and the shear failure strain, ε_f, and GIIC(shear CZMlaws). The deviation in the CZM parameters showed a reduced scatter between CZM laws of the same adhesive.

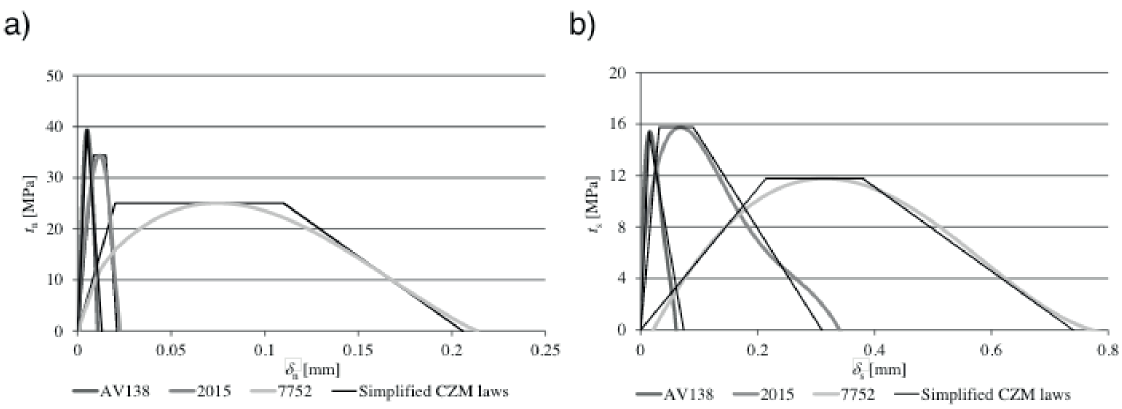

Fig.8 - Comparison of representative tn-dn (a) and ts-ds (b) curves for each of the adhesives.

4.2 Strength prediction

The average values of tensile and shear CZM parameters were used to build triangular, trapezoidal and linear-exponential tensile and shear CZM laws for each of the three adhesives. These laws were subsequently input in numerical simulations of double-lap joints respecting the principles depicted in Section 3.1 as a validation of the obtained CZM laws by the J-integral/direct method. Fig. 9 compares the experimental and numerical maximum load (Pm) values as function of LO for the three CZM laws and the adhesives Araldite® AV138 (a), Araldite® 2015 (b) and Sikaforce® 7752.

For the joints bonded with the Araldite® AV138, the best results are obtained by the triangular CZM law, followed by the trapezoidal CZM law, while the linear-exponential CZM law clearly under estimates Pm. These results are justified by the brittleness of the adhesive, which was attested by the properties depicted in Table 1 and tensile and shear CZM laws represented in Fig. 8. The average absolute error (considering the four LO values) is 0.56% for the triangular CZM law, 1.17% for the trapezoidal CZM law and 2.79% for the linear-exponential CZM law. The largest % errors always occur for LO=12.5 mm, disregarding the CZM law type. Differently to this adhesive, for the joints bonded with the Araldite® 2015, the best predictions were attained with the trapezoidal CZM law, which is consistent with the moderate degree of ductility of this adhesive. The triangular and especially the linear-exponential CZM laws under predict the experiments. The average deviations of absolute values, considering all LO values, are 2.00% (triangular law), 1.03% (trapezoidal law) and 2.76% (linear-exponential law). For this particular adhesive, it was found that, from LO=37.5 mm, Pm is ruled by the adherends' yielding/tensile net failure rather than the adhesive.

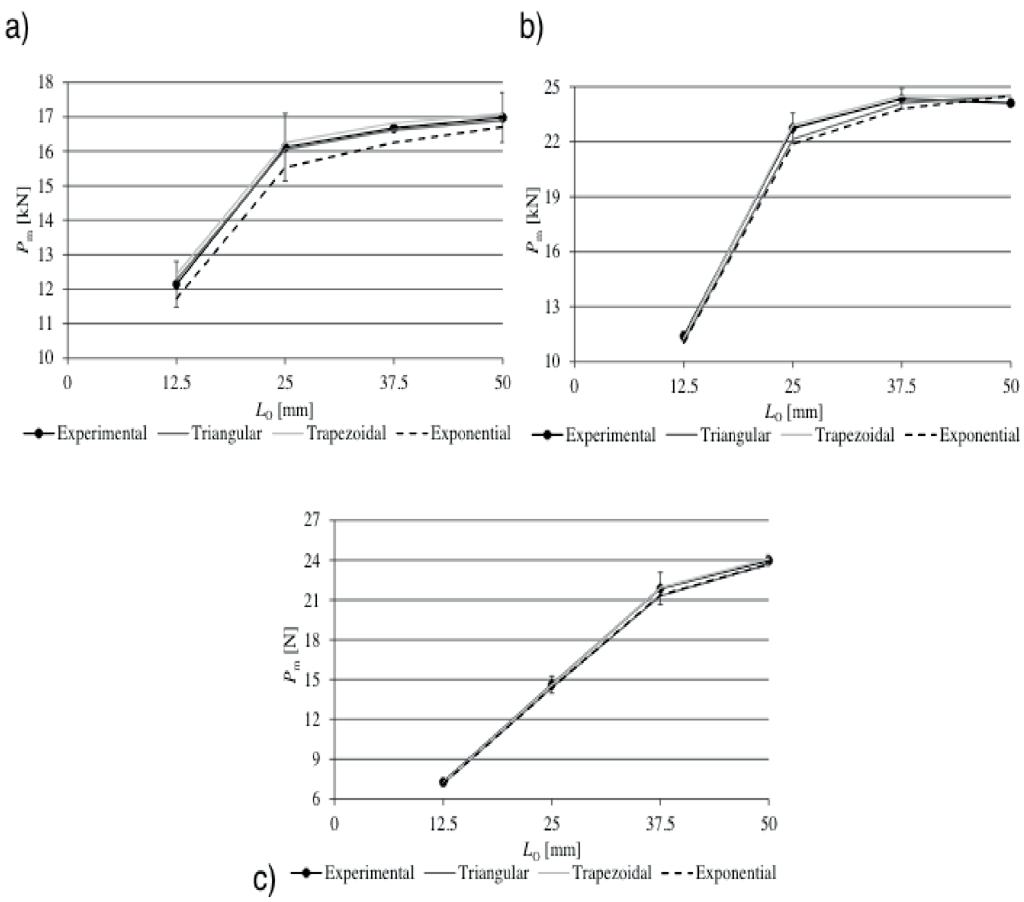

Fig. 9 - Comparison between the experimental and numerical Pm values as function of LO for the three CZM laws and the adhesives Araldite® AV138 (a), Araldite® 2015 (b) and Sikaforce® 7752 (c).

Because of the high ductility of the Sikaforce® 7752, for the joints bonded with this adhesive the trapezoidal CZM law gives the best approximation, while the triangular and linear-exponential CZM laws present identical under predictions. The average % deviations of absolute values of each adhesive are 1.73% (triangular law), 0.36% (trapezoidal law) and 1.73% (linear-exponential law). For L_O=50 mm, Pm is governed by the adherends' yielding or tensile net failure. Globally, for the tested geometrical conditions, no significant errors would be made by using an improper CZM law, i.e., a CZM law that is not the best fit to the tensile and shear CZM laws of the respective adhesive obtained by the direct method. However, this is the result of two factors: (1) the range of L_O values used is this work is relatively limited and (2) for all adhesives, tensile adherend failure or at least adherends plasticization affected the Pm results such that, for the higher Pm values, the joints' failure was no longer ruled by the adhesive but by the adherend's yielding. In fact, in a previous work (Campilho, Banea, et al., 2013) considering triangular and trapezoidal CZM shapes to model single-lap joints with L_O values up to 80 mm revealed that higher L_O values in joints with non-yielding composite adherends can give differences of over 10% compared to the experiments if the CZM law does not closely follow the adhesive's behaviour. Thus, depending on the required accuracy for the results, the choice of the correct CZM law type may be of importance.

5 I CONCLUSIONS

The main objective of this work was the assessment of different CZM shapes in predicting the behaviour of a mixed-mode joint geometry bonded with adhesives of distinct ductility, after estimating the tensile and shear CZM laws of the adhesives by the direct method. The DCB and ENF specimens were considered to obtain the tensile and shear CZM laws of the adhesives, respectively. The obtained CZM laws were highly consistent for each loading/adhesive combination. In both loading modes, the Araldite® AV138 was best modelled by a triangular CZM law due to its brittleness, while the ductile Araldite® 2015 and Sikaforce® 7752 showed a better fit with trapezoidal CZM laws. Validation of these CZM laws was undertaken with a mixed-mode geometry (double-lap joint) considering the same three adhesives and varying L_O values. Previous to the analysis, the double-lap joints' strength revealed to be highly dependent on the adhesive type. Actually, the Araldite® AV138 showed a similar Pm value to the Araldite® 2015 for L_O =12.5 mm, but it was unable to increase Pm with L_O by a significant amount on account of being very brittle (oppositely to the Araldite® 2015). The joints bonded with the Sikaforce® 7752 showed a much smaller Pm value for L_O=12.5 mm because of the smaller strengths, but the ductility of this adhesive enabled to increase Pm with L_O in a practically linear relation. All Pm-L_O curves for the three adhesives were affected by the inner adherend's failure or at least plasticization for the higher L_O values. Regarding the Pm comparison between the experiments and numerical predictions, the deviations were small for all CZM laws, although the best results closely followed the previously mentioned agreement regarding the experimental and approximated CZM laws. Thus, for the tested geometrical conditions, no significant errors would be made by using an improper CZM law. However, it should be noted that, depending on the geometry of the joints and adherends' behaviour, the error of using a non-consistent CZM law shape to the behaviour of the adhesive to be simulated can result in non-negligible deviations to the real joints' behaviour.

REFERENCES

ALFANO, G.; CRISFIELD, M. A. Finite element interface models for the delamination analysis of laminated composites: mechanical and computational issues. **International Journal for Numerical Methods in Engineering,** v. 50, n. 7, p. 1701-1736, 2001. ISSN 1097-0207. Disponível em: < http://dx.doi.org/10.1002/nme.93 >.

AZEVEDO, J. C. S. et al. Cohesive law estimation of adhesive joints in mode II condition. **Theoretical and Applied Fracture Mechanics**, v. 80, p. 143-154, 2015.

CAMPILHO, R. D. S. G. et al. Modelling of single-lap joints using cohesive zone models: Effect of the cohesive parameters on the output of the simulations. **The Journal of Adhesion**, v. 88, n. 4-6, p. 513-533, 2012/04/01 2012. ISSN 0021-8464. Disponível em: < http://dx.doi.org/10.1080/00218464.2012.660834 >. Acesso em: 2015/01/21.

______. Modelling adhesive joints with cohesive zone models: effect of the cohesive law shape of the adhesive layer. **International Journal of Adhesion and Adhesives**, v. 44, p. 48-56, 7// 2013. ISSN

0143-7496. Disponível em: < http://www.sciencedirect.com/science/article/pii/S0143749613000353 >.

CAMPILHO, R. D. S. G. et al. Strength prediction of single- and double-lap joints by standard and extended finite element modelling. **International Journal of Adhesion and Adhesives**, v. 31, n. 5, p. 363-372, 7// 2011. ISSN 0143-7496. Disponível em: < http://www.sciencedirect.com/science/article/pii/S0143749611000273 >.

CAMPILHO, R. D. S. G.; DE MOURA, M. F. S. F.; DOMINGUES, J. J. M. S. Using a cohesive damage model to predict the tensile behaviour of CFRP single-strap repairs. **International Journal of Solids and Structures**, v. 45, n. 5, p. 1497-1512, 3/1/ 2008. ISSN 0020-7683. Disponível em: < http://www.sciencedirect.com/science/article/pii/S002076830700412X >.

CAMPILHO, R. D. S. G. et al. Adherend thickness effect on the tensile fracture toughness of a structural adhesive using an optical data acquisition method. **International Journal of Adhesion and Adhesives**, v. 53, p. 15-22, 9// 2014. ISSN 0143-7496. Disponível em: < http://www.sciencedirect.com/science/article/pii/S0143749614000165 >.

______. Adhesive thickness effects of a ductile adhesive by optical measurement techniques. **International Journal of Adhesion and Adhesives**, v. 57, p. 125-132, 3// 2015. ISSN 0143-7496. Disponível em: < http://www.sciencedirect.com/science/article/pii/S0143749614002097 >.

CAMPILHO, R. D. S. G. et al. Fracture toughness determination of adhesive and co-cured joints in natural fibre composites. **Composites Part B: Engineering**, v. 50, p. 120-126, 7// 2013. ISSN 1359-8368. Disponível em: < http://www.sciencedirect.com/science/article/pii/S1359836813000437 >.

CAMPILHO, R. D. S. G. et al. Adhesively Bonded Repair Proposal for Wood Members Damaged by Horizontal Shear Using Carbon-Epoxy Patches. **The Journal of Adhesion**, v. 86, n. 5-6, p. 649-670, 2010/06/16 2010. ISSN 0021-8464. Disponível em: < http://dx.doi.org/10.1080/00218464.2010.484318 >.

CONSTANTE, C. J.; CAMPILHO, R. D. S. G.; MOURA, D. C. Tensile fracture characterization of adhesive joints by standard and optical techniques. **Engineering Fracture Mechanics,** v. 136, p. 292-304, 3// 2015. ISSN 0013-7944. Disponível em: < http://www.sciencedirect.com/science/article/pii/S0013794415000508 >.

FANECO, T. M. S. et al. Strength and fracture characterization of a novel polyurethane adhesive for the automotive industry. **Journal of Testing and Evaluation**, v. Submitted, 2015.

FERNANDES, T. A. B. et al. Adhesive selection for single lap bonded joints: Experimentation and advanced techniques for strength prediction. **The Journal of Adhesion**, v. 91, n. 10-11, p. 841-862, 2015/10/03 2015. ISSN 0021-8464. Disponível em: < http://dx.doi.org/10.1080/00218464.2014.994703 >. Acesso em: 2015/08/29.

GOYAL, V. K.; JOHNSON, E. R.; GOYAL, V. K. Predictive strength-fracture model for composite bonded joints. **Composite Structures**, v. 82, n. 3, p. 434-446, 2// 2008. ISSN 0263-8223. Disponível em: < http://www.sciencedirect.com/science/article/pii/S0263822307000268 >.

HAN, J.; SIEGMUND, T. Cohesive zone model characterization of the adhesive Hysol EA-9394. **Journal of Adhesion Science and Technology**, v. 26, n. 8-9, p. 1033-1052, 2012/05/01 2012. ISSN 0169-4243. Disponível em: < http://www.tandfonline.com/doi/abs/10.1163/016942410X550003 >. Acesso em: 2015/08/25.

JI, G. et al. Effects of adhesive thickness on global and local Mode-I interfacial fracture of bonded joints. **International Journal of Solids and Structures**, v. 47, n. 18–19, p. 2445-2458, 9// 2010. ISSN 0020-7683. Disponível em: < http://www.sciencedirect.com/science/article/pii/S0020768310001769 >.

JIANG, W.-G. et al. A concise interface constitutive law for analysis of delamination and splitting in composite materials and its application to scaled notched tensile specimens. **International**

Journal for Numerical Methods in Engineering, v. 69, n. 9, p. 1982-1995, 2007. ISSN 1097-0207. Disponível em: < http://dx.doi.org/10.1002/nme.1842 >.

LEFFLER, K.; ALFREDSSON, K. S.; STIGH, U. Shear behaviour of adhesive layers. **International Journal of Solids and Structures**, v. 44, n. 2, p. 530-545, 1/15/ 2007. ISSN 0020-7683. Disponível em: < http://www.sciencedirect.com/science/article/pii/S0020768306001466 >.

LEITÃO, A. C. C.; CAMPILHO, R. D. S. G.; MOURA, D. C. Shear Characterization of Adhesive Layers by Advanced Optical Techniques. **Experimental Mechanics**, v. 56, p. 493-506, 2015/12/02 2016. ISSN 0014-4851. Disponível em: < http://dx.doi.org/10.1007/s11340-015-0111-4 >.

LI, J. et al. Experimental study of adhesively bonded CFRP joints subjected to tensile loads. **International Journal of Adhesion and Adhesives**, v. 57, p. 95-104, 3// 2015. ISSN 0143-7496. Disponível em: < http://www.sciencedirect.com/science/article/pii/S014374961400205X >.

PANDYA, K. C.; WILLIAMS, J. G. Measurement of cohesive zone parameters in tough polyethylene. **Polymer Engineering & Science**, v. 40, n. 8, p. 1765-1776, 2000. ISSN 1548-2634. Disponível em: < http://dx.doi.org/10.1002/pen.11308 >.

RICE, J. R. A path independent integral and the approximate analysis of strain concentration by notches and cracks. **Journal of Applied Mechanics**, v. 35, n. 2, p. 379-386, 1968. ISSN 0021-8936. Disponível em: < http://dx.doi.org/10.1115/1.3601206 >.

TURON, A. et al. An engineering solution for mesh size effects in the simulation of delamination using cohesive zone models. **Engineering Fracture Mechanics**, v. 74, n. 10, p. 1665-1682, 7// 2007. ISSN 0013-7944. Disponível em: < http://www.sciencedirect.com/science/article/pii/S0013794406003808 >.

VALOROSO, N. et al. Identification of mode-I cohesive parameters for bonded interfaces based on DCB test. **Engineering Fracture Mechanics**, v. 104, p. 56-79, 5// 2013. ISSN 0013-7944. Disponível em: < http://www.sciencedirect.com/science/article/pii/S0013794413000507 >.

VOLKERSEN, O. Die nietkraftoerteilung in zubeanspruchten nietverbindungen konstanten loschonquerschnitten. **Luftfahrtforschung**, v. 15 p. 41-47, 1938.

ZHU, Y.; LIECHTI, K. M.; RAVI-CHANDAR, K. Direct extraction of rate-dependent traction–separation laws for polyurea/steel interfaces. **International Journal of Solids and Structures,** v. 46, n. 1, p. 31-51, 1/1/ 2009. ISSN 0020-7683. Disponível em: < http://www.sciencedirect.com/science/article/pii/S0020768308003351 >.

SOBRE OS ORGANIZADORES

Henrique Ajuz Holzmann: Professor da Universidade Tecnológica Federal do Paraná (UTFPR). Graduação em Tecnologia em Fabricação Mecânica e Engenharia Mecânica pela Universidade Tecnológica Federal do Paraná. Mestre em Engenharia de Produção pela Universidade Tecnológica Federal do Paraná Doutorando em Engenharia e Ciência do Materiais pela Universidade Estadual de Ponta Grossa. Trabalha com os temas: Revestimentos resistentes a corrosão, Soldagem e Caracterização de revestimentos soldados.

João Dallamuta: Professor da Universidade Tecnológica Federal do Paraná (UTFPR). Engenheiro de Telecomunicações pela UFPR. Especialista em Inteligência de Mercado pela FAE Business School. Mestre em Engenharia pela UEL. Trabalha com os temas: Inteligência de Mercado, Sistemas Eletrônicos e Gestão Institucional.

Ricardo Vinicius Bubna Biscaia: Professor da Universidade Tecnológica Federal do Paraná (UTFPR). Graduado em Engenharia Mecânica pela Universidade Tecnológica Federal do Paraná. Mestre em Engenharia Mecânica pela Universidade Tecnológica Federal do Paraná Doutorando em Engenharia de Produção pela UTFPR. Trabalha com os temas: análise microestrutural e de microdureza de ferramentas de usinagem, modelo de referência e processo de desenvolvimento de produto e gestão da manutenção.

ÍNDICE REMISSIVO

T

U

V

Agência Brasileira do ISBN
ISBN 978-85-7247-798-7
9 788572 477987